Atmos. Chem. Phys. Discuss., 9, 8857–8902, 2009
www.atmos-chem-phys-discuss.net/9/8857/2009/

Atmospheric Chemistry and Physics Discussions

This discussion paper is/has been under review for the journal *Atmospheric Chemistry and Physics (ACP)*. Please refer to the corresponding final paper in *ACP* if available.

Isoprene oxidation by nitrate radical: alkyl nitrate and secondary organic aerosol yields

A. W. Rollins[1], A. Kiendler-Scharr[3], J. Fry[1], T. Brauers[3], S. S. Brown[4], H.-P. Dorn[3], W. P. Dubé[4], H. Fuchs[4], A. Mensah[3], T. F. Mentel[3], F. Rohrer[3], R. Tillmann[3], R. Wegener[3], P. J. Wooldridge[1], and R. C. Cohen[1,2]

[1]Department of Chemistry, University of California Berkeley, Berkeley, CA 94720, USA
[2]Department of Earth and Planetary Science, University of California Berkeley, Berkeley, CA 94720, USA
[3]Institute of Chemistry and Dynamic of the Geosphere, Forschungszentrum Jülich, Germany
[4]Chemical Sciences Division, NOAA Earth System Research Laboratory, Boulder, CO, USA

Received: 27 February 2009 – Accepted: 17 March 2009 – Published: 3 April 2009

Correspondence to: Ronald C. Cohen (rccohen@berkeley.edu)

Published by Copernicus Publications on behalf of the European Geosciences Union.

Abstract

Alkyl nitrates and secondary organic aerosol (SOA) produced during the oxidation of isoprene by nitrate radicals has been observed in the SAPHIR chamber. We find the yield of nitrates is 70±8% from the isoprene+NO_3 reaction, and the yield for secondary dinitrates produced in the reaction of primary isoprene nitrates with NO_3 is 40±20%. We find an effective rate constant for reaction of NO_3 with the group of first generation oxidation products to be 7×10^{-14} cm^3 s^{-1}. At the low total organic aerosol concentration in the chamber (max ≈0.6 $\mu g\,m^{-3}$) we observed a mass yield (ΔSOA mass/Δisoprene mass) of 2% for the entire 16 h experiment. However a comparison of the timing of the observed SOA production to a box model simulation of first and second generation oxidation products shows that the yield from the first generation products was <0.2% while the further oxidation of the initial products leads to a yield of 10% (defined as $\Delta SOA/\Delta isoprene^{2x}$ where $\Delta isoprene^{2x}$ is the mass of isoprene which reacted twice with NO_3). The SOA yield of 10% is consistent with equilibrium partitioning of highly functionalized C_5 products of isoprene oxidation.

1 Introduction

Isoprene (2-methyl-1,3-butadiene) is globally the most abundant non-methane volatile organic compound (VOC), with an estimated emission of 440–660 Tg C/year (Guenther et al., 2006). Total non-methane VOC emissions are estimated at 1150 Tg C/year biogenic (Guenther et al., 1995) and 186 Tg C/year anthropogenic (Olivier et al., 2005) making isoprene the source of 34%–51% of the non-methane organic carbon emitted to the Earth's atmosphere. The combined factors of its source strength and high reactivity to atmospheric oxidants (OH, O_3, and NO_3), make isoprene a major factor in the chemistry of the troposphere. As a result, tropospheric O_3 and aerosol burdens and distributions are highly sensitive to the products of isoprene chemistry (e.g., Chameides et al., 1988; Thornton et al., 2002; Henze and Seinfeld, 2006; Wu et al., 2007).

ACPD

9, 8857–8902, 2009

Isoprene emissions are near zero at night when nitrate radical chemistry is traditionally thought to be of primary importance. However, isoprene emitted during the day is observed to persist after sundown when NO_3 concentrations begin to increase (Starn et al., 1998; Stroud et al.; Steinbacher et al., 2005), and theoretical arguments suggest that NO_3 can be important in shaded forest canopies near NO_x (NO_x=NO+NO_2) sources even during daytime (Fuentes et al., 2007). NO_3 has been measured during the day in polluted urban areas (Geyer et al., 2003a) and new developments in NO_3 instrumentation allowing for sub ppt sensitivity are beginning to reveal the potential importance of NO_3 – VOC chemistry during the day (Brown et al., 2005). Global estimates made with GEOS-Chem suggest that ≈6% of the total isoprene oxidation occurs by NO_3 (Ng et al., 2008) while regionally in areas of high NO_x that are collocated with isoprene sources it has been shown to be 22% or higher (Brown et al., 2009).

Alkyl nitrates ($RONO_2$) formed from reactions of isoprene with NO_3 represent ≈50% of the total nitrate production in isoprene rich regions, with likely consequences for tropospheric O_3 production (Horowitz et al., 1998; von Kuhlmann et al., 2004; Fiore et al., 2005; Horowitz et al., 2007; Wu et al., 2007). Photochemical (OH) oxidation of isoprene has been shown to produce aerosol with yields that are small (1–3%) (Kroll et al., 2005, 2006) compared to yields from other biogenic VOC's, but due to the source strength of isoprene this could be the single most significant source of SOA on Earth (Henze and Seinfeld, 2006; Zhang et al., 2007; Ng et al., 2008). SOA from the reaction of isoprene with NO_3 has been recently studied (Ng et al., 2008), with significant yields observed (4.3–23.8%). The nitrate radical reacts primarily with unsaturated VOC's and therefore is a particularly effective oxidant for many biogenic compounds. Isoprene which has two double bonds, can react with NO_3 at each bond, and the products of both oxidation steps can affect both NO_x and NO_y (NO_y=NO_x+organic nitrates+NO_3+2×N_2O_5+HNO_2+HNO_3+particulate nitrate) partitioning as well as SOA formation. However, there is little detailed information about the second step in the isoprene oxidation sequence.

Kinetics of the first step in isoprene oxidation by NO_3 are well established. The

rate constant has been measured by a number of investigators using various methods (Atkinson et al., 1984; Benter and Schindler, 1988; Dlugokencky and Howard, 1989; Barnes et al., 1990; Berndt and Boge, 1997; Wille et al., 1991; Suh et al., 2001) and the recommended rate constant at 298 K is 6.8×10^{-13} molecule^{-1} cm^3 s^{-1} (Atkinson et al., 2006). The mechanism for the reaction is addition of NO_3 to one of the double bonds, mainly at the C1 position. Theoretical and experimental studies are in good agreement that the main product of the reaction in the presence of oxygen will be a C_5 nitrooxycarbonyl. Minor products include C_5 hydroxynitrates, C_5 nitrooxyhydroperoxides, methyl vinyl ketone (MVK) and methacrolein (MACR) (Barnes et al., 1990; Skov et al., 1992; Ng et al., 2008). Ng et al. (2008) also identified some of the gas and particle phase products of the further oxidation of these initial products. SOA was observed to form from both first generation and second generation products. Reaction of the C_5-hydroxynitrate with NO_3 was more correlated with production of SOA than was the reaction of the other major C_5 products. Highly functionalized C_{10} peroxides were also identified in the gas and particle phases. Ng et al. (2008) concluded that SOA in this system is produced more efficiently by RO_2+RO_2 reactions than by RO_2+NO_3 reactions.

In this work we report a chamber experiment on the reaction of isoprene+NO_3 performed with lower levels of isoprene and NO_x than in prior experiments. High precision measurements of both gas phase and particle phase products have been made, including especially detailed observations of nitrogen species. NO, NO_2, NO_3, N_2O_5, and total alkyl nitrates ($\Sigma RONO_2$) were observed This unique set of measurements provides a new measure of the alkyl nitrate yield and allows us to estimate the reactivity of the initial oxidation products, strengthening our understanding of the mechanism by which gas and aerosol products are produced in the ambient environment.

2 Experimental

The experiment was conducted in the SAPHIR (Simulation of Atmospheric PHotochemistry In a large Reaction Chamber) chamber in Jülich, Germany. The reaction chamber is a double walled 120 μm Teflon-FEP cylindrical bag, 5 m in diameter and 18 m long providing a volume of $\approx$270 m^3. The chamber is housed in an aluminum structure with shutters that can be left open to outside lighting, or closed to simulate nighttime chemistry. During experiments the chamber is overpressured by 40–60 Pa with respect to the ambient pressure, and the space between the two FEP sheets is continually flushed with high purity N_2. These measures isolate the air inside the chamber from outside air. Air sampled from the chamber during experiments is replaced with synthetic dry air to maintain the positive pressure. A mixing fan inside the chamber continuously stirs the gas in the chamber to maintain a spatially uniform mixture with a mixing time of 2–3 min. SAPHIR has been described in detail elsewhere (Bossmeyer et al., 2006; Rohrer et al., 2005; Wegener et al., 2007).

2.1 Instrumentation

This experiment was conducted on 18 July 2007 during an intercomparison campaign focused on measurements of NO_3 (Dorn et al., 2009) and N_2O_5 (Apodaca et al., 2009), during which ten different instruments for measurement of NO_3 and/or N_2O_5 were co-located at the SAPHIR chamber. NO_3 and N_2O_5 measurements were found to be in agreement to ±10% for almost all of the instruments throughout the campaign. Figures and analysis in this paper make use of Cavity Ringdown Spectroscopy (CaRDS) measurements reported by the NOAA group (Brown et al., 2001; Dubé et al., 2006) with accuracies of +12%/−9% for NO_3 and +11%/−8% for N_2O_5 (Fuchs et al., 2008). Measurements of isoprene were obtained by Proton Transfer Reaction-Mass Spectrometry (PTR-MS), and Gas Chromatography with Flame Ionization Detector (GC-FID). Volatile organic compounds (VOC) including MVK, MACR and methyl ethyl ketone (MEK) were also measured with GC-FID. NO and NO_2 were measured with a Chemiluminescence

(CL) instrument equipped with a photolytic converter (ECO Physics CLD TR 780). NO_2 as well as the higher nitrogen oxide classes total peroxy nitrates (ΣPNs), total alkyl and multifunctional nitrates ($\Sigma RONO_2$) were also measured by Thermal Decomposition-Laser Induced Fluorescence (TD-LIF) (Thornton et al., 2000; Day et al., 2002). Ozone was measured with a UV Photometer (ANSYCO O341M), as well as with a CL detector (ECO Physics CLD AL 700) modified as described by Ridley et al. (1992). Both O_3 instruments were in good agreement and figures in this paper show the CL measurements.

Aerosol size distribution, surface area, volume, and total number density were obtained with a Scanning Mobility Particle Sizer (SMPS) (TSI model 3936L85) and Condensation Particle Counter (CPC) (TSI model 3785) with time resolutions of 7 min and 20 s, respectively. A high resolution (Δm/m=250 ppm at *m/z*=100, DeCarlo et al., 2006) aerosol mass spectrometer (Aerodyne HR-ToF-AMS) was operated to measure the aerosol chemical composition, providing data every 2 min. The AMS was connected to the SAPHIR chamber via a stainless steel tube designed to minimize losses in the sampling line. Details of the AMS are described in (Canagartna et al., 2007). The high resolution (HR) capabilities of the AMS can distinguish between chemically different fragments at the same nominal mass (i.e. NO^+ and CH_2O^+ at *m/z*=30) when signal to noise is high enough. HR analysis was used to exclude the non nitrogen containing fragments from the nominally nitrate peaks at *m/z*=30 and 46, as well as to ensure the other major peaks normally considered organic did not contain nitrogen.

2.2 Experiment description

The chamber was prepared by flushing for 12.5 h with clean synthetic air at a rate of 75 m^3/h. Starting at 06:20 UTC, the chamber was loaded with trace gasses to meet the intended experimental conditions (relative humidity=57%, ethane 5.5 ppb as a tracer for dilution, CO 500 ppm as an OH scavenger, isoprene 9.6 ppb, and NO_2 16 ppb, see Fig. 1). In addition we added ammonium sulfate seed aerosol (3.5 $\mu g/m^3$). At 08:50, O_3 (37 ppb) was added initiating the production of NO_3. After 5 h of reaction time the

chemistry was accelerated with the addition of 23 ppb NO_2 and 43 ppb O_3, and then approximately 1 h after the isoprene was fully consumed another 11 ppb of isoprene was added. The slow reaction of O_3 and NO_2 generated NO_3 radicals throughout the experiment, consuming the majority of the isoprene. We calculate that throughout the experiment ≈90% of the isoprene reacted with NO_3 and ≈10% with O_3. The GC-FID measurements of ethane were fitted to an exponential decay with a rate constant of $k_{dil}=1.39\times10^{-5}\,s^{-1}$, which was applied to all species in the box model to account for dilution.

2.3 Modeling

The Kinetic PreProcessor (KPP V2.1) (Sandu and Sander, 2006) was used to produce code for kinetic box model simulations of the chamber experiment. Two sets of simulations were run. In one set KPP input was provided by the Master Chemical Mechamism (MCM V3.1) (Saunders et al., 2003). In another set of simulations the MCM isoprene+NO_3 degradation scheme was modified and optimized to reproduce the chamber observations, leaving the isoprene+O_3 scheme identical to that in the MCM. The full reaction set used in this second scheme is listed in Table 1, and both mechanisms are shown schematically in Fig. 2 for comparison. This second mechanism includes two main deviations from the MCM: firstly, the yield to form alkyl nitrates as the first generation oxidation products of isoprene+NO_3 is less than 100%, and secondly, these initial oxidation products retain a double bond to which NO_3 can add electrophilically, eventually forming additional multifunctional nitrates.

Details of the chemistry included in the modified model are as follows:

- *Inorganic chemistry:* the inorganic reactions and rates are taken directly from the MCM website[1].
- *VOC chemistry:* MVK and MACR are assumed to be produced with yields of 3.5%

[1] http://mcm.leeds.ac.uk/MCM/

each from isoprene+NO_3, as was previously reported (Kwok et al., 1996) and these yields are held fixed in the simulations. HO_x is assumed to be produced by 80% of the RO_2 reactions, which is a rough approximation consistent with the semi-explicit model used by Horowitz et al. (2007). OH and HO_2 are not distinguished because the 500 ppm CO in the chamber immediately converts OH to HO_2.

The only measurement we made of the other carbon products of isoprene oxidation is the $\Sigma RONO_2$. We reduce the model complexity by only distinguishing these oxidation products by their -ONO_2 content and whether they have undergone a second oxidizing reaction with NO_3 or O_3. NIT1 (Table 1, Fig. 2) is representative of all first generation oxidation products which have one -ONO_2 group. The branching ratio to form NIT1 is a tunable parameter in the model. The group of species represented by NIT1 is reactive towards NO_3 and O_3. The effective rate for reaction of NO_3 with this group of unsaturated species is also tunable, and is fit to be 7.0×10^{-14} molecules^{-1} cm^3 s^{-1} to achieve the best agreement between modeled and measured NO_3 and N_2O_5 (see Sect. 3.1). The nitrate radical which reacts with NIT1 is presumed to lead to the production of additional -ONO_2 functionality (NIT3, either di-nitrate or 2 organic nitrate molecules), or be converted to NO_2 or HNO_3 leaving the original -ONO_2 group attached to a different carbon backbone (NIT2). The branching ratio between formation of NIT2 and NIT3 is the final tunable parameter in the model. The reaction of NIT1 with O_3 makes NIT4 which is also treated as an unspecified $RONO_2$. The modeled $\Sigma RONO_2$ is therefore NIT1+NIT2+2 × NIT3+NIT4+NISOPO2+NIT1NO3OO.

Because the primary oxidation product of isoprene+NO_3 is believed to be 4-nitrooxy-3-methyl-2-butanal, we use the reaction rates of the structurally similar 2-methyl-2-butene as a reference for the ratio of the reaction rates with O_3 and NO_3 (both rates taken from MCM). Thus, $k_{O_3}=4.3\times10^{-5}\times k_{NO_3}$. The choice to use 4-nitrooxy-3-methyl-2-butanal as the reference compound for these rates has a small impact on the outcome of the model because the O_3 reaction is much

slower than the NO_3 reaction. The O_3 Reaction R9 accounts for 7% of the consumption of the NIT1 species throughout the entire model run, while during the short SOA growth period (14:30–16:15) it is only 4%. Using methacrolein as the reference compound increases these values to 26% and 17%, respectively.

– *Peroxy radicals:* peroxy radicals in the model are generated by reactions of each double bond of isoprene with NO_3. All peroxy radical (RO_2) reaction rates are taken directly from MCM. The initial isoprene nitrate peroxy radical+RO_2 rate is $1.30\times10^{-12}\,cm^3\,s^{-1}$, and this rate is used also for all second generation RO_2+RO_2 reactions. All RO_2+NO_3 and RO_2+HO_2 reactions proceed at standard MCM rates of $2.5\times10^{-12}\,cm^3\,s^{-1}$ and $2.3\times10^{-11}\,cm^3\,s^{-1}$, respectively (see Table 1). The yield for product formation is modeled to be the same regardless of the peroxy radical reaction partner, and the products of all peroxy radical reactions are only distinguished by whether a stable alkyl nitrate or NO_2 is formed. For example, two isoprene peroxy radicals could form a C_{10} peroxide, or two C_5 products. These product channels are not tracked in the model because the only observable and therefore modeled quantities are NO_x, NO_3, N_2O_5 and $\Sigma RONO_2$.

3 Gas phase products

We first describe the observations from the chamber and show that different time periods uniquely constrain some of the model parameters. Two distinct chemical environments dominated the chemistry in the chamber at three different time periods. These time periods are referred to by their UTC hour and are most obvious in the observations of NO_3 and N_2O_5 (Fig. 1c).

1. 08:00–14:30: during the initial phase the isoprene concentration was high and isoprene dominated the consumption of nitrate radicals. The NO_3 production rate ranged from $0.56\,ppt\,s^{-1}$ ($2.0\,ppb\,h^{-1}$) at 08:00 to $0.16\,ppt\,s^{-1}$ ($0.58\,ppb\,h^{-1}$) at

14:30. At any given time >90% of the NO_3 loss was due to reaction with isoprene, with the majority of the balance being to reaction with oxidation products. Reaction of peroxy radicals is predominately with other peroxy radicals and hydroperoxy radicals. RO_2+NO_3 accounts for <5% of RO_2 reactions.

2. 14:30–16:15: during this second phase, the isoprene concentration decreased rapidly to zero and reaction with the initial oxidation products was a much more important sink for NO_3. Between UTC 15:18 and 16:15 reaction with these initial oxidation products accounted for more than half of the total NO_3 reactivity. VOC's generated by NO_3 oxidation of both double bonds of isoprene rapidly accumulated. RO_2+NO_3 also accounted for a larger fraction of the peroxy radical reactions, peaking at ≈40–50% of total peroxy radical loss.

3. 16:15–24:00: during the third phase an additional 11 ppb isoprene was added. Isoprene again was the dominant sink of NO_3, suppressing both the production of the doubly oxidized products of isoprene and RO_2+NO_3 reactions.

3.1 Optimized model parameters

As previously discussed, three of the model parameters have been adjusted to minimize differences in the model-measurement comparison. These are: 1) branching ratios for the formation of alkyl nitrates vs NO_2 from the isoprene+NO_3 reaction, 2) reaction rate of 1st generation oxidation products with NO_3, and 3) branching ratios for formation of alkyl nitrates and NO_2 from the reaction of NO_3 with the first generation oxidation products. Wall losses of NO_3 and N_2O_5 were determined in a pervious VOC and aerosol free experiment. A loss rate of organic nitrates to the chamber walls is determined to be 2.2×10^{-5} s^{-1} by a best fit of the $\Sigma RONO_2$ data and model at the end of the experiment when changes in $\Sigma RONO_2$ are the most sensitive to this process. Model optimization of the free parameters was achieved in the following order:

1. *Branching ratio #1:* stable nitrates result from addition of NO_3 and O_2 to iso-

ACPD
9, 8857–8902, 2009

prene followed by a radical-radical reaction that produces a closed shell product through either an abstraction reaction followed by a cleavage, or a recombination of the radicals (Fig. 2). The branching ratio (Y_{AN1}) to form alkyl nitrates from isoprene+NO_3, is defined as the fraction of isoprene+NO_3 reactions that eventually form stable nitrates:

$$Y_{AN1} = \frac{\Delta\Sigma RONO_2}{\Delta isoprene} \quad (1)$$

This ratio would be equal to $\Delta RONO_2/\Delta NO_3$ if $\Delta NO_3 = \Delta isoprene$, i.e. in the absence of another NO_3 sink. An initial attempt was made to evaluate this branching ratio directly from changes in the NO_3, N_2O_5 and $\Sigma RONO_2$ observations during second addition of isoprene to the chamber. This addition lead to a prompt consumption of a known amount of NO_3 and N_2O_5, and subsequent production of alkyl nitrates and NO_2. However, because the NO_3 concentration was high relative to RO_2, we calculate that $RO_2+NO_3 \rightarrow RO+NO_2+O_2$ accounted for ≈15–25% of the total RO_2 reactions, meaning that on the order of 20% of the sudden change in NO_3 radicals was due to the reaction with peroxy radicals, not isoprene. Due to the uncertainty in the reaction rate for the specific peroxy radicals with NO_3 it is not possible to precisely calculate the contribution of this reaction to the ΔNO_3. For the initial phase of the experiment however the concentration of NO_3 was so low that the rate of NO_3+RO_2 is minor compared to RO_2+RO_2 and RO_2+HO_2, and uncertainties in the reaction rates other than NO_3+isoprene result in a small uncertainty in the branching ratio.

To evaluate the yields of alkyl nitrates and NO_2 we therefore varied this yield in simulations run over the time period 07:00–13:00 UTC (Fig. 3). A yield 70±8% alkyl nitrates and 30% NO_2 was found to minimize the accumulated residuals between model and measurements of $RONO_2$ and NO_2 over this time period.

2. *Alkyl nitrate+NO_3 reaction rate:* with the branching ratios for the first generation products fixed at 70% and 30% for alkyl nitrates and NO_2, re-

spectively, the time period 14:00–16:15 UTC was used to fit the rate coefficient for reaction of the lumped species NIT1+NO_3. A rate coefficient of $7\times10^{-14}\pm3\times10^{-14}$ molecules^{-1} cm^{3}s^{-1} was found to be optimal (Fig. 3) based on minimizing residuals in comparison of modeled and observed NO_3+N_2O_5.

3. *Alkyl nitrate+NO_3 products:* using the optimized branching ratios for isoprene+NO_3 and the optimized reaction rate, the branching ratio to form alkyl nitrates or NO_2 from the second oxidation step was investigated. Focusing on the time period 14:00–16:15 UTC when the isoprene was depleted so that $RONO_2$+NO_3 was the primary sink of NO_3, we examined the yield in 20% increments (Fig. 4). The model and measurements are in best agreement for a yield of 40%±20%. We note that a yield of greater than 0% for NO_2 produces a significant positive bias in the model runs and the yield for NO_2 for this reaction is therefore set to 0% for the final run. This implies that the second oxidation step has a high yield to form HNO_3 directly.

Figure 5 shows a comparison between the MCM model, and the model optimized in this work for modeled $\Sigma RONO_2$, NO_2 NO_3 and N_2O_5. Generally, the MCM overpredicts NO_3, N_2O_5 and alkyl nitrates, and underpredicts NO_2.

Our observation of alkyl nitrate formation (70±10%) is equivalent to previously reported yields (60%–80%), within the combined experimental errors (Barnes et al., 1990; Skov et al., 1992; Perring et al., 2009). The fact that multiple experiments conducted under different conditions (concentrations of isoprene and oxidants differing by more than a factor of 100) have all produced high yields of alkyl nitrates implies that the yield is robust and relatively insensitive to the peroxy radical chemistry, and supports findings that the isoprene+NO_3 reaction is possibly the single strongest source of alkyl nitrates in the atmosphere (Horowitz et al., 2007).

MACR, MVK and methyl ethyl ketone (MEK) were observed in small yields. Approximately 70% of the observed MVK and 80% MACR were calculated to be from the reaction of isoprene with ozone, and the remainder is consistent with yields of 2–4%

for both MVK and MACR from NO_3+isoprene. Production of 0.9 ppb MEK was also observed by 24:00 UTC. The observations of the yields of MACR and MVK are consistent with previous observations. Barnes et al. (1990) reported an observable but small yield of MACR. Skov et al. (1992) report MACR below their FTIR detection limit (<5%). Kwok et al. (1996) measured the production of MVK and MACR with GC-FID and reported yields of 3.5% for both MVK and MACR. Perring et al. (2009) observed a 7% yield of the sum of MVK and MACR using PTR-MS. Skov et al. (1992) and Perring et al. (2009) measured product yields by adding isoprene to a chamber that was initially charged with ppm levels of N_2O_5. Kwok et al. (1996) added isoprene first as we did, but then injected N_2O_5 in ppm steps. All of these experiments would have resulted in much larger NO_3/RO_2 ratio than in the experiment reported on here. These similar yet small yields of MVK and MACR observed in vastly different radical regimes are not surprising, supporting the conclusion that the yields of these products are primarily determined by the position at which O_2 adds to the alkyl radical generated by isoprene+NO_3 as opposed to the peroxy radical reaction partner. The observation of 0.9 ppb MEK at the end of the experiment is surprising. It seems that this product would have appeared in the FTIR detection scheme of Skov et al. (1992), however they do not report observing it. The mechanism responsible for the MEK in our experiments is unclear and might have been an interference from a different compound with the same GC retention time.

The rate constant that we find for the reaction of the first generation oxidation products with NO_3 (7×10^{-14} molecules^{-1} cm^{3}s^{-1}) can be compared to known rate constants for compounds that are likely to be structurally similar. The observations that ≈40% of this reaction generates an alkyl nitrate, while ≈60% of the nitrogen does not reappear in any of our measurements indicates that the reaction occurred by ≈40% addition of NO_3 to a double bond, and ≈60% abstraction of the aldehydic hydrogen, with rate constants of $0.4\times7\times10^{-14}=2.8\times10^{-14}$ molecules^{-1} cm^3 s^{-1} and $0.6\times7\times10^{-14}=4.2\times10^{-14}$ molecules^{-1} cm^3 s^{-1} for these two respective reactions. 3-methyl-2-butene-1-ol (MBO) is a unsaturated alcohol structurally similar to the hydroxynitrate produced by the isoprene+NO_3. The reaction rate constant for MBO has been

ACPD
9, 8857–8902, 2009

measured as 1×10^{-12} molecules^{-1} cm^3 s^{-1} (Noda et al., 2002). While the effects of nitrate substitutions has not been studied on the reactions of alkenes with NO_3, the electronegative nitrate group should be expected to slow the reaction. For example, in the case of the electrophilic OH addition to a double bond, the C_5-hydroxynitrate reaction rate constant would be predicted to be a factor of 5 slower than that for MBO (Kwok and Atkinson, 1995). Scaling the MBO reaction by a factor of 5 yields a rate constant of 2×10^{-13} molecules^{-1} cm^3 s^{-1}, ten times faster than our fitted value of 2.8×10^{-14} molecules^{-1} cm^3 s^{-1}. The presumed rate constant for hydrogen abstraction of 4.2×10^{-14} molecules^{-1} cm^3 s^{-1} is on the fast end of the range that has been measured for aldehydes with NO_3. D'Anna et al. (2001) measured a rate constant of 2.68×10^{-14} molecules^{-1} cm^3 s^{-1} for the reaction of 2-methylbutanal, which differs from the C_5 hydroxycarbonyl only by a nitrate substitution at the δ carbon. We caution that these comparisons are only intended only to be rough, as we only are considering what are believed to be the highest yield isomers of the isoprene+NO_3 reactions. Further, the measured products from the initial reaction only account for 77% of the primary products ($\Sigma RONO_2$+MVK+MACR) and it may be reaction of one of the unresolved initial products that consumes most of this NO_3 and produces SOA. However, this would contradict the findings of Ng et al. (2008) who report at least 2 nitrogen atoms in almost all of the molecules forming SOA from this system.

3.2 Peroxy radical fate

The relative concentration of peroxy radical reaction partners RO_2, HO_2 and NO_3 can lead to differences in observed yields of i.e. peroxides, hydroperoxides and nitrates between experiments. Figure 6 shows the modeled contributions of these three radicals to the total RO_2 reactions throughout the experiment. For the majority of the experiment the RO_2 fate is almost entirely dominated by reaction with peroxy and hydroperoxy radicals. NO_3 is modeled to be a significant reaction partner for peroxy radicals for a brief period of time in the middle of the experiment when the isoprene concentration was

zero and the nitrate radical production rate was high (≈1.5 ppt s^{-1}). During this time, a large concentration of NO_3 accumulated (max≈150 ppt) at the same time that RO_2 and HO_2 production decreased.

While it would be interesting to use this experiment to help clarify the role of nighttime peroxy radical reactions in tropospheric chemistry, direct comparison of the modeled peroxy radical chemistry to the nighttime atmosphere is not conclusive. Box models simulating nighttime chemistry are in disagreement as to whether or when NO_3+RO_2 reactions can compete with RO_2+RO_2 and RO_2+HO_2 as a sink for RO_2. At least two studies have concluded that in polluted environments NO_3 can be an important sink for RO_2 (Geyer et al., 2003b; Vaughan et al., 2006), while Bey et al. (2001) conclude that this process is insignificant. One of the reasons for this discrepancy may be the lack of detailed knowledge surrounding RO_2+RO_2 and RO_2+NO_3 reaction rates. Our experiment does not address constraints to these rates.

We do note that model calculations (both the modified model and MCM) suggest that HO_2 dominates the fate of peroxy radicals in the chamber. If all RO_2+HO_2 reactions formed a hydroperoxide via RO_2+HO_2→ROOH, than the majority of the oxidation products would be hydroperoxides instead of carbonyls. Ng et al. (2008) conducted a chamber study with higher total radical concentrations, but presumably similar ratios between HO_2 and RO_2. They observed a ratio of carbonylnitrate: nitrooxy hydroperoxide of ≈4–5. These combined results suggest that either the rate of RO_2+RO_2 is much faster relative to RO_2+HO_2 than used in our calculations, or that the yield for hydroperoxides from RO_2+HO_2 may be significantly less than 100%. Laboratory (Hasson et al., 2004; Jenkin et al., 2007; Crowley and Dillon, 2008) and theoretical (Hasson et al., 2005) studies have shown that while the hydroperoxide yield from small peroxy radicals such as methyl peroxy and ethyl peroxy is near 100%, larger more substituted peroxy radicals especially of the form R(O)OO may form alcohols or OH in high yields from the reaction with HO_2. Photochemical box models have also been shown to more accurately reproduce field data if RO_2+HO_2 reactions are not chain terminating sinks of HO_x (e.g., Thornton et al., 2002; Lelieveld et al., 2008). Thus, the yield of ROOH

from RO_2+HO_2 reactions is currently an open question.

4 Aerosol

Figure 1 shows the raw AMS signal. The AMS indicated some brief initial increase in SOA with the injection of O_3, but this production did not continue throughout the experiment and our analysis focuses on the more significant growth between 14:00 and 17:00 UTC. The number density of particles followed a monotonic exponential decay with a lifetime of 3.7 h throughout the experiment, presumably due to wall losses. We assume that the observed SOA is due the combined effects of SOA production and wall loss and in Fig. 7 we show the SOA corrected for this loss. Secondary organic aerosol was observed to increase rapidly during the phase of the experiment when the isoprene concentration was low and the NO_3 concentration was at its peak. The rapid growth of SOA observed uniquely in the presence of high NO_3 concentration indicated that SOA formation was initiated by NO_3 oxidation rather than O_3. The fact that this growth also took place when isoprene concentration was at a minimum indicated that this SOA was generated upon reaction of NO_3 with one of the initial isoprene oxidation products as opposed to isoprene itself. A final mass yield in the traditional sense

$$Y = \frac{\Delta\text{organic aerosol mass}}{\Delta\text{isoprene mass}} \quad (2)$$

of 2% was observed.

Figure 7 shows the change in AMS organic aerosol corrected for chamber dilution and wall loss (green), the modeled net amount of isoprene consumed by NO_3 (blue), and the modeled net amount of isoprene nitrates (produced by the isoprene+NO_3 reaction with a 70% yield) consumed by reaction with NO_3 (extent of Reaction R5 from Table 1, red line). The blue curve shows Δisoprene (μg/m^3) and the red curve shows the moles of second generation oxidation products multiplied by the molecular weight of isoprene. We define this quantity as $\Delta\text{isoprene}^{2x}$ because it is the mass concentration

ACPD
9, 8857–8902, 2009

of isoprene which reacted two times with NO_3. Mass yields with respect to isoprene can be read for the first and second oxidation steps by comparing these lines to the AMS data. By 14:00 UTC, approximately 12.5 $\mu g\,m^{-3}$ isoprene has reacted with NO_3. SOA production over the pervious 4 h is within the noise of the AMS ($\approx$0.02 $\mu g\,m^{-3}$), indicating that the direct yield of SOA from the isoprene+NO_3 reaction is <0.2%. The mass yield of SOA from the reaction of NO_3 with the intermediate isoprene nitrates however is approximately 10% based on the observed final production of 0.8 $\mu g\,m^{-3}$ SOA (1.4 $\mu g\,m^{-3}$ at 24:00 – 0.6 $\mu g\,m^{-3}$ at 10:00) and the calculated of 8 $\mu g\,m^{-3}$ isoprene reacted through this channel (i.e. $\Delta isoprene^{2x}$=8 $\mu g\,m^{-3}$).

The TD-LIF instrumentation observes the sum of gas and aerosol organic nitrates. Figure 8 shows the changes in TD-LIF signal and AMS nitrate, with both measurements averaged to 15 min resolution. We observed an increase of $\approx$4 $\mu g\,m^{-3}$ total organic nitrate coincident with 0.12 $\mu g\,m^{-3}$ aerosol nitrate. This indicates that $\approx$3% of the organic nitrate produced in the second oxidation step partitioned to the particle phase. Of the final SOA products which exist in gas/particle equilibrium, the molecular yield can be calculated by scaling the mass yield (10%) by the relative molecular weights of isoprene and of the SOA. For example, assuming particle/gas equilibrium if the primary SOA component were a C_5-dinitrate-diol ($C_5H_{10}O_8N_2$) with MW=226, the fraction of this molecule in the particle phase would be 10%×68/226=3% which is in agreement with our nitrate partitioning observation.

4.1 SOA composition

The design of the gas phase model used in this study was primarily motivated by accurately calculating the partitioning of NO_y throughout two stages of isoprene oxidation, and thus species were lumped according to their nitrate content. However, other studies (Barnes et al., 1990; Skov et al., 1992; Ng et al., 2008; Perring et al., 2009) have distinguished hydroxynitrates, carbonylnitrates, and peroxynitrates as the majority of the oxidation products. In Fig. 9 we consider physical properties including expected

SOA yields of some of the specific molecules that may be responsible for SOA produced from the isoprene+NO_3 system. These expected yields are then compared to the calculated 10% mass yield, and 3% molar yield from the second oxidation step.

This figure depicts the evolution of isoprene oxidation products through two stages of oxidation by nitrate radical, assuming that in each step the reaction takes place by addition of NO_3 to one of the C=C bonds. For simplicity, we consider secondary oxidation products produced by the reaction of NO_3 with the C_5 hydroxynitrate, as the consumption of this product was highly correlated with SOA formation in the study of Ng et al. (2008). Similar second generation structures could be arrived at from reactions of the C_5 carbonylnitrate, and the predicted vapor pressures of these products are a factor of 6–8 higher than for the analogous hydroxynitrate. Although multiple isomers of each molecule are possible, we show only one of each for simplicity. The vapor pressure of these molecules is determined primarily by the number of carbon atoms and the molecular functionalities, various isomers should have similar vapor pressures. For each molecule we show the molecular weight (Da, black), estimated vapor pressure P_L^0 (Pa, blue) effective saturation concentration C^* ($\mu g\,m^{-3}$, green). From the effective saturation we calculate the fraction of this molecule residing in the particle phase in the presence of $0.6\,\mu g\,m^{-3}$ organic aerosol (red), which was the maximum observed OA concentration in this experiment. Vapor pressures are estimated using the group contribution method (Pankow and Asher, 2008) which has been demonstrated to estimate these values to within a factor of 2 for 456 atmospheric compounds spanning 14 orders of magnitude in P_L^0. The vapor pressure is related to an equilibrium partitioning coefficient (K) and to the effective saturation concentration (C^*) by

$$K = \frac{1}{C^*} = \frac{760\,R\,T}{\mathrm{MW_{om}} 10^6 \xi P_L^0} \quad (3)$$

with R being the ideal gas constant ($8.206\times10^{-5}\,m^3\,atm\,mol^{-1}\,K^{-1}$), T is the temperature (K), $\mathrm{MW_{om}}$ is the mean molecular weight of the organic aerosol ($g\,mol^{-1}$) and ξ is the activity coefficient of the species in the organic aerosol phase, which is typically

assumed to be 1 (Odum et al., 1996). While the mean molecular weight of the organic aerosol in this experiment is likely >200 g mol^{-1}, here we assume MW$_{om}$=150 g mol^{-1} as is typically used in calculations of atmospheric aerosol. The fraction of a given molecule i which is residing in the OA phase (Y_i) is then calculated under these assumptions using the relationship between C^*, the particle phase (C_p) and gas phase (C_g) concentrations of species, and the ambient OA concentration (M_0):

$$\frac{1}{C^*} = \frac{C_p}{C_g M_0} \tag{4}$$

$$Y_i = \frac{M_0/C^*}{1 + M_0/C^*} \tag{5}$$

At low concentrations of aerosol, the yield calculated as a function of vapor pressure is highly sensitive to both M_0 and MW$_{om}$. In Fig. 10 we illustrate how changes in these values would have an effect on the partitioning of the C$_5$-dinitrate-diol (P_L^0=9.7×10^{-5} Pa). In Fig. 9 we calculate that for MW$_{om}$=150 and M_0=0.6 μg m^{-3} (the maximum observed in this work before correction for losses), Y_i=9%. If the OA is completely composed of this substance (MW$_{om}$=226), the yield would be ≈6%. Generally, given uncertainties in MW$_{om}$ and M_0 we find that equilibrium partitioning predicts yields of ≪1% for the first generation products, ≈5–20% for the second generation C$_5$ products, and >95% for the C$_{10}$ peroxides. Considering the factor of two uncertainty in the vapor pressures of the oxidation products and the assumption that ξ=1, we find these predicted yields reasonably close to the 3% molar yield observed and conclude that the primary components of the aerosol are most likely C$_5$ second generation oxidation products. The yields that would have been observed if the aerosol was primarily composed of first generation oxidation products or highly functionalized peroxides are well outside the range of our data.

Figure 11 shows the AMS nitrate vs. AMS organic signals from UTC 14:15–24:00. A linear fit to the data indicates that the ratio of nitrate:organic of the SOA (on a mass

basis) was approximately 0.18 for the entire period, with the highest ratio of 0.20 occuring between 14:15 and 16:36 UTC. The production of SOA with a nitrate:organic ratio of 0.18 could in principle be due to condensation either of a single nitrate containing organic compound with this ratio, or by co-condensation of multiple oxidation products. In Fig. 9 (purple numbers) we have estimated the nitrate:organic mass ratio that would be observed for the presumed second generation products, assuming that $RONO_2$ fragments in the AMS as R (organic) and ONO_2 (nitrate) and each are detected with equal efficiency. The calculated values are shown in purple. All molecules have nitrate:organic mass ratios >1, much too large to explain the observations. Fragmentation of organic nitrates $RONO_2 \rightarrow RO+NO_2$ on the AMS heater is likely, which would reduce these ratios somewhat. For example, the dinitrate-diol structure of MW 226 would in this case have a nit:org ratio of 0.66 instead of 1.05. This however is still much higher than our observed 0.18. The discrepancy here could be explained by a number of mechanisms, including: 1) co-condensation of nitrate and non-nitrate organics, 2) polymerization of the nitrate peroxy radicals with non-nitrate containing species, or some other addition of non-nitrate functional groups to the isoprene oxidation products, 3) underestimation of the nitrate content in the aerosol, or 4) release of nitrogen upon condensation of organic nitrates.

Isoprene (C_5H_8) and nitrate radical (NO_3), respectively, have molecular weights of 68, and 62. If a single molecule is forming the SOA through the addition of one nitrate radical followed by the polymerization of isoprene units, this would be somewhere between 5 and 6 isoprene units (0.18 and 0.15 nitrate/organic mass, respectively). Even if we assume that oxidation of each double bond of isoprene adds 2 oxygens to the mass ($C_5H_8O_4$, MW=132) this would require at least two fully oxidized isoprenes per nitrate group. Laboratory studies have observed the formation of polymers from isoprene in SOA (Jang et al., 2002; Kalberer et al., 2004; Surratt et al., 2006; Müller et al., 2008) by various mechanisms and some of these may be possibilities here.

An internal isomerization of the δ-alkoxy radical formed by NO_3 addition to isoprene at the 1 position via a 6 membered ring is also a possibility for adding non-nitrate

functionality to the oxidation products (Fig. 12). This could lead to a slight decrease in the nitrate:organic ratio: 0.93 vs. the 1.2 for example if the second double bond of the two products shown in Fig. 12 reacts again with NO_3. Estimates of the relative estimated rates of isomerization and hydrogen abstraction of the alkoxy radical also suggest that this may be a significant pathway (Atkinson, 2007). The production of this molecule as a main product of the isoprene+NO_3 reaction would not be in conflict with some previous product studies for which organic nitrate standards were not available and for which the product chemical structure has been deduced based on the existence of carbonyl and nitrate peaks in FTIR spectra. Ng et al. (2008) however do not report significant yields of this product, even though it would have been likely to be detected by their CIMS with comparable efficiency to other products that are reported.

Ng et al. (2008) reported many highly nitrated structures observed in both the gas phase, and on filter samples produced in their isoprene+NO_3 experiment. Although an AMS nitrate:organic ratio for this experiment was not reported, all of the structures observed with their CIMS and filter extraction TOFMS have much higher nitrate:organic ratios than we measured. Furthermore, as we have observed in the initial reaction, and as is well founded for many alkene NO_3 reactions, the yield of organic nitrate formation from these reactions is high. The continued oxidation of double bond containing isoprene oxidation products is expected to lead to the formation of organic nitrates. Therefore it seems most reasonable that the condensing species were similar to the C_5 dinitrate species in Fig. 9. Our data can neither confirm nor deny the possibility of release of NO_x during SOA formation due to rapid changes in total NO_2 which would have been only contributed to in a minor way from this process. While AMS nitrogen:carbon and oxygen:carbon ratios have been verified for nitrogen containing compounds including amines, amides and phenols, (Aiken et al., 2007) similar results have not been reported for molecules containing $RONO_2$ groups, leaving open the possibility that organic nitrate content is underestimated.

5 Atmospheric implications

Our observations indicate that the formation of SOA from isoprene+NO_3 under typical concentrations of OA will rely on the extent to which both double bonds of isoprene are oxidized. Here, we observed oxidation of both bonds via reaction with NO_3. However, the exchange of a nitrate group with a hydroxy group has a minor affect on the effective saturation concentration, thus we expect that reaction with NO_3 followed by reaction with OH or vice versa would produce a similar aerosol yield. To consider the extent to which these second oxidation steps will take place in the atmosphere, we compare the lifetime of the initial oxidation products to reaction with OH and NO_3 to their lifetimes with respect to wet and dry deposition.

MCM uses a rate constant for 4-nitrooxy-3-methyl-2-butanal with OH of 4.16×10^{-11} molecules^{-1} cm^3 s^{-1}. This rate is roughly consistent with those measured by Treves and Rudich (2003) for unsaturated hydroxyalkyl nitrates. At an average daytime concentration of 2×10^6 molecules/cm^3 this would give a lifetime to OH of 3.3 h, indicating these compounds generated at night by NO_3 chemistry remaining through the next morning would be consumed by reaction with OH early in the day.

We found an effective rate constant for the initial oxidation products with NO_3 of 7.0×10^{-14} molecules^{-1} cm^3 s^{-1}. Nighttime NO_3 concentrations are highly variable ranging from 0 to hundreds of pptv, and depend on the availability of NO_x. In a recent study Brown et al. (2009) show that the first generation daytime isoprene oxidation products MVK and MACR, are found at ppb levels along with 50–100 ppt NO_3. This range of NO_3 concentrations would yield 3.1–1.6 h for lifetimes of isoprene nitrates.

We use the method of Brimblecombe and Dawson (1984) to estimate the wet deposition rate of the first generation oxidation products. This method has been used previously to estimate the wet removal rate of hydroxy-nitrate isoprene oxidation products (Shepson et al., 1996). Henry's law coefficients at 283 K of 4-nitrooxy-3-methyl-2-butanal (2.3×10^4 M/atm) and 4-nitrooxy-3-methyl-2-butanol (3.3×10^5 M/atm) were calculated using the SPARC online calculator (Hilal et al., 2003, 2004). Using the same

ACPD
9, 8857–8902, 2009

assumptions for mid-latitude meteorology as Shepson et al. (1996) and Brimblecombe and Dawson (1984), we use these Henry's law constants to calculate rainout rates of $2.3\times10^{-6}\,s^{-1}$ for the carbonyl-nitrate and $5.5\times10^{-6}\,s^{-1}$ for the hydroxy-nitrate. These rates imply rainout lifetimes of these species of 5 and 2.1 days, respectively, both which are too slow to compete with the lifetime to reaction.

Lifetimes to dry deposition are perhaps less well constrained, although we note that loss to dry deposition is unlikely at night because most of the isoprene+NO_3 reaction will take place above the nocturnal boundary layer. Dry deposition velocities (v_d) of HNO_3 have been reported in the range of 2–4 $cm\,s^{-1}$ (Seinfeld and Pandis, 1998; Farmer and Cohen, 2008), while reported PAN deposition velocities range from 0.25–0.8 $cm\,s^{-1}$ (Turnipseed et al., 2006; Garland and Penkett, 1976; Farmer and Cohen, 2008; Wolfe et al., 2009). Multi-functional nitrate deposition velocity have been measured by Shepson et al. (1996) and Farmer and Cohen (2008) at 0.4 $cm\,s^{-1}$ and 2.0 $cm\,s^{-1}$, respectively, and inferred from NO_y fluxes by Munger et al. (1996) ranging from 0.5 $cm\,s^{-1}$ at night to 2 $cm\,s^{-1}$ during the day. Assuming the same scale height as we use for the wet deposition calculation (2.3 km) the lifetime ($\tau=Z/v_d$ where Z=scale height) for v_d of 0.25–2.0 $cm\,s^{-1}$ would be 10–1.3 days if it were important.

These estimates of wet and dry deposition lifetimes of the carbonyl- and hydroxy-nitrate first generation oxidation products of isoprene are significantly longer than lifetimes to chemical reaction by average daytime OH concentrations, and NO_3 concentration greater than 10 ppt. For NO_3 above 10 ppt the first generation oxidation products are likely to react with NO_3 at night converting them to condensible species, but on timescales longer than the rapid reaction of isoprene with NO_3 that has been observed immediately after sunset. For much smaller NO_3 concentrations, transport at night, daytime deposition or OH oxidation will dominate the fate of these nitrates.

6 Summary and conclusions

We have observed the reaction of isoprene with nitrate radicals at atmospherically relevant concentrations of VOC and oxidants (9.6 ppb isoprene, 16 ppb NO_2, 37 ppb O_3). A modified version of the MCM was used to evaluate the yields for alkyl nitrates from the reaction of isoprene with NO_3 (70%) and for the subsequent reaction of the first generation oxidation products with NO_3 (20–60%). NO_3 observations which were significantly lower than predicted by the MCM were used to determine an effective rate constant for reaction of the group of first generation oxidation products with NO_3. We observed that SOA is formed from the isoprene/NO_3 system, but at low organic aerosol concentration (<1 $\mu g/m^3$), only when both double bonds of isoprene are oxidized. Using the modified MCM, we estimate that the SOA mass yield of isoprene which reacts two times with NO_3 is 10% and show that this yield is consistent with equilibrium partitioning of the expected oxidation products. Modeling also indicates an inconsistency between the current estimations of the relative magnitudes of the rate constants for RO_2+RO_2 vs. RO_2+HO_2, and the expectation that RO_2+HO_2→ ROOH with a 100% yield. The AMS data reported much less nitrate content than would be expected from these structures, and we therefore conclude that either some additional chemistry was responsible for the chemical content of the SOA, or the aerosol nitrogen content is higher than measured.

Acknowledgements. The Berkeley authors were supported by NSF ATM-0639847 and NSF ATM-0511829. The authors would like to thank the SAPHIR NO3 intercomparison campaign team for organizing and administering the experiments in June 2007 at Forschungszentrum Jülich. This work was a joint activity of the European Community Network of Excellence ACCENT, grant no. GOCE CT-2004-505337 and the EUROCHAMP project.

References

Aiken, A., DeCarlo, P., and Jimenez, J.: Elemental Analysis of Organic Species with Electron Ionization High-Resolution Mass Spectrometry, Anal. Chem., 79, 8350–8358, 2007. 8877

Apodaca, R. L., Simpson, W., Ball, S. M., Brauers, T., Brown, S. S., Cohen, R. C., Crowley, J., Dorn, H.-P., Dubé, W. P., Fry, J. L., Fuchs, H., Haseler, R., Heitmann, U., Kato, S., Kajii, Y., Kiendler-Scharr, A., Kleffmann, J., Labazan, I., Matsumoto, J., Nishida, S., Rollins, A. W., Tillmann, R., Wahner, A., Wegener, R., and Wooldridge, P. J.: Intercomparison of N_2O_5 sensors using SAPHIR reaction chamber, in preparation, 2009. 8861

Atkinson, R.: Rate constants for the atmospheric reactions of alkoxy radicals: An updated estimation method, Atmos. Environ., 41, 8468–8485, 2007. 8877

Atkinson, R., Aschmann, S. M., Winer, A. M., and Pitts, J. N. J.: Kinetics of the Gas-Phase Reactions of NO_3 Radicals with a Series of Dialkenes, Cycloalkenes, and Monoterpenes at 295±1 K, Environ. Sci. Technol., 18, 370–375, 1984. 8860

Atkinson, R., Baulch, D. L., Cox, R. A., Crowley, J. N., Hampson, R. F., Hynes, R. G., Jenkin, M. E., Rossi, M. J., Troe, J., and IUPAC Subcommittee: Evaluated kinetic and photochemical data for atmospheric chemistry: Volume II – gas phase reactions of organic species, Atmos. Chem. Phys., 6, 3625–4055, 2006, http://www.atmos-chem-phys.net/6/3625/2006/. 8860

Barnes, I., Bastian, V., Becker, K. H., and Tong, Z.: Kinetics and Products of the Reactions of NO_3 with Monoalkenes, Dialkenes, and Monoterpenes, J. Phys. Chem., 94, 2413–2419, 1990. 8860, 8868, 8869, 8873

Benter, T. and Schindler, R. N.: Absolute rate coefficients for the reaction of NO_3 radicals with simple dienes, Chem. Phys. Lett., 145, 67–70, 1988. 8860

Berndt, T. and Boge, O.: Gas-Phase Reaction of NO_3 Radicals With Isoprene: A Kinetic and Mechanistic Study, Int'l. J. Chem. Kin., 29, 755–765, 1997. 8860

Bey, I., Aumont, B., and Toupance, G.: A modeling study of the nighttime radical chemistry in the lower continental troposphere 1. Development of a detailed chemical mechanism including nighttime chemistry, J. Geophys. Res., 106, 9959–9990, 2001. 8871

Bossmeyer, J., Brauers, T., Richter, C., Rohrer, F., Wegener, R., and Wahner, A.: Simulation chamber studies on the NO_3 chemistry of atmospheric aldehydes, Geophys. Res. Lett., 33, L18810, doi:10.1029/2006GL026778, 2006. 8861

Brimblecombe, P. and Dawson, G. A.: Wet Removal of Highly Soluble Gases, J. Atmos. Chem.,

2, 95–107, 1984. 8878, 8879
Brown, S. S., Stark, H., Circiora, S. J., and Ravishankara, A. R.: In-situ measurement of atmospherc NO_3 and N_2 O_5 via cavity ring-down spectroscopy, Geophys. Res. Lett, 28, 3227–3230, 2001. 8861
Brown, S. S., Osthoff, H. D., Stark, H., Dube, W. P., Ryerson, T. B., Warneke, C., de Gouw, J. A., Wollny, A. G., Parrish, D. D., Fehsenfeld, F. C., and Ravishankara, A. R.: Aircraft observations of daytime NO_3 and N_2O_5 and their implications for tropospheric chemistry, J. Photoch. Photobio. A, 176, 270–278, 2005. 8859
Brown, S. S., deGouw, J. A., Warneke, C., Ryerson, T. B., Dubé, W. P., Atlas, E., Weber, R. J., Peltier, R. E., Neuman, J. A., Roberts, J. M., Swanson, A., Flocke, F., McKeen, S. A., Brioude, J., Sommariva, R., Trainer, M., Fehsenfeld, F. C., and Ravishankara, A. R.: Nocturnal isoprene oxidation over the Northeast United States in summer and its impact on reactive nitrogen partitioning and secondary organic aerosol, Atmos. Chem. Phys. Discuss., 9, 225–269, 2009, http://www.atmos-chem-phys-discuss.net/9/225/2009/. 8859, 8878
Canagartna, M., Jayne, J., Jimenez, J., Allan, J., Alfarra, M., Zhang, Q., Onaxch, T., Drewnick, F., Coe, H., Middlebrook, A., Delia, A., Williams, L., Trimborn, A., Northway, M., DeCarlo, P., Kolb, C., Davidovits, P., and Worsnop, D.: Chemical and microphysical characteriation of ambient aerosols with the aerodyne aerosol mass spectrometer, Mass Spectrom. Rev., 26, 185–222, 2007. 8862
Chameides, W. L., Lindsay, R. W., Richardson, J., and Kiang, C. S.: The Role of Biogenic Hydrocarbons in Urban Photochemical Smog: Atlanta as a Case Study, Science, 241, 1473–1475, 1988. 8858
Dillon, T. J. and Crowley, J. N.: Direct detection of OH formation in the reactions of HO2 with $CH_3C(O)O_2$ and other substituted peroxy radicals, Atmos. Chem. Phys., 8, 4877–4889, 2008, http://www.atmos-chem-phys.net/8/4877/2008/. 8871
D'Anna, B., Andresen, O., Gefen, Z., and Nielsen, C. J.: Kinetic study of OH and NO_3 radical reactions with 14 alihatic aldehydes, Phys. Chem. Chem. Phys., 3, 3057–3063, doi:10.1039/b103623h, 2001. 8870
Day, D. A., Wooldridge, P. J., Dillon, M., Thornton, J. A., and Cohen, R. C.: A thermal dissociation laser-induced fluorescence instrument for in situ detection of NO_2, peroxy nitrates, alkyl nitrates, and HNO_3, J. Geophys. Res., 107(D6), 4046, doi:10.1029/2001JD000779, 2002.

8862
DeCarlo, P. F., Kimmel, J. R., Trimborn, A., Northway, M. J., Jayne, J. T., Aiken, A. C., Gonin, M., Fuhrer, K., Horvath, T., Docherty, K. S., Worsnop, D. R., and Jimenez, J. L.: Field-Deployable, High-Resolution, Time-of-Flight Aerosol Mass Spectrometer, Anal. Chem., 78, 8281–8289, 2006. 8862
Dlugokencky, E. J. and Howard, C. J.: Studies of NO_3 Radical Reactions with Some Atmospheric Organic Compounds at Low Pressures, J. Phys. Chem, 93, 1091–1096, 1989. 8860
Dorn, H.-P., Apodaca, R. L., Ball, S. M., Brauers, T., S., B. S., Cohen, R. C., Crowley, J., Dubé, W. P., Fry, J. L., Fuchs, H., Haseler, R., Heitmann, U., Jones, R., Kato, S., Kajii, Y., Kiendler-Scharr, A., Labazan, I., Matsumoto, J., Meinen, J., Nishida, S., Platt, U., Rohrer, R., Rollinw, A. W., Ruth, A. A., Schlosser, E., Schuster, G., Schillings, A., Simpson, W., Thieser, J., Tillmann, R., Varma, R., Venables, D., Wahner, A., Wegener, R., and Wooldridge, P. J.: Intercomparison of NO_3 measurement techniques at the simulation chamber SAPHIR, in preparation, 2009. 8861
Dubé, W. P., Brown, S. S., Osthoff, H. D., Nunley, M. R., Circiora, S. J., Paris, M. W., McLaughlin, R. J., and Ravishankara, A. R.: Aircraft instrument for simultaneous, in situ measurement of NO_3 and N_2 O_5 via pulsed cavity ring-down spectroscopy, Rev. Sci. Inst., 77, 034101, doi:10.1063/1.2176058, 2006. 8861
Farmer, D. K. and Cohen, R. C.: Observations of HNO_3, SAN, SPN and NO_2 fluxes: evidence for rapid HO_x chemistry within a pine forest canopy, Atmos. Chem. Phys., 8, 3899–3917, 2008, http://www.atmos-chem-phys.net/8/3899/2008/. 8879
Fiore, A. M., Horowitz, L. W., Purves, D. W., Levy, H. I., Evans, M. J., Want, Y., Li, Q., and Yantosca, R. M.: Evaluating the contribution of changes in isoprene emissions to surface ozone trends over the eastern United States, J. Geophys. Res., 110, D12303, doi:10.1029/2004JD005485, 2005. 8859
Fuchs, H., Dubé, W., Ciciora, S., and Brown, S.: Determination of Inlet Transmission and Conversion Efficiencies for in Situ Measurements of the Nocturnal Nitrogen Oxides, NO_3, N_2O_5 and NO_2 via Pulsed Cavity Ring-Down Spectroscopy, Anal. Chem., 80, 6010–6017, 2008. 8861
Fuentes, J. D., Wang, D., Bowling, D. R., Potosnak, M., Monson, R. K., Goliff, W. S., and Stockwell, W. R.: Biogenic Hydrocarbon Chemistry within and Above a Mixed Desciduous Forest, J. Atmos. Chem., 56, 165–185, doi:10.1007/s10874-006-9048-4, 2007. 8859

Garland, J. A. and Penkett, S. A.: Absorption of peroxy acetyl nitrate and ozone by natural surfaces, Atmos. Environ., 10, 1127–1131, 1976. 8879

Geyer, A., Alicke, B., Ackermann, R., Martinez, M., Harder, H., Brune, W., di Carlo, P., Williams, E., Jobson, T., Hall, S., Shetter, R., and Stutz, J.: Direct observations of daytime NO_3: Implications for urban boundary layer chemistry, J. Geophys. Res., 108(D12), 4368, doi: 10.1029/2002JD002967, 2003a. 8859

Geyer, A., Bächmann, K., Hofzumahaus, A., Holland, F., Konrad, S., Klüpfel, T., Pätz, H.-W., Perner, D., Mihelcic, D., Schäfer, H.-J., Volz-Thomas, A., and Platt, U.: Nighttime formation of peroxy and hydroxyl radicals during the BERLIOZ campaign: Observations and modeling studies, J. Geophys. Res., 108(D4), 8249, doi:10.1029/2001JD000656, 2003b. 8871

Guenther, A., Hewitt, C. N., Erickson, D., Fall, R., Geron, C., Graedel, T., Harley, P., Klinger, L., Lerdau, M., McKay, W. A., Pierce, T., Scholes, B., Steinbrecher, R., Tallamraju, R., Taylor, J., and Zimmerman, P.: A global model of natural volatile organic compound emissions, J. Geophys. Res., 100, 8873–8892, doi:10.1029/94JD02950, 1995. 8858

Guenther, A., Karl, T., Harley, P., Wiedinmyer, C., Palmer, P. I., and Geron, C.: Estimates of global terrestrial isoprene emissions using MEGAN (Model of Emissions of Gases and Aerosols from Nature), Atmos. Chem. Phys., 6, 3181–3210, 2006, http://www.atmos-chem-phys.net/6/3181/2006/. 8858

Hasson, A. S., Tyndall, G. S., and Orlando, J. J.: A Product Yield Study of the Reaction of HO_2 Radicals with Ethyl Peroxy ($C_2H_5O_2$), Acetyl peroxy ($CH_3C(O)O_2$), and Acetonyl Peroxy ($CH_3C(O)CH_2O_2$) Radicals, J. Phys. Chem. A., 108, 5979–5989, 2004. 8871

Hasson, A. S., Kuwata, K. T., Arroyo, M. C., and Petersen, E. B.: Theoretical studies of the reaction of hydroperoxy radicals (HO_2) with ethyl peroxy ($CH_3CH_2O_2$), acetyl peroxy ($CH_3C(O)O_2$), and acetonyl peroxy ($CH_3C(O)CH_2O_2$) radicals, J. Photoch. Photobio. A, 176, 218–230, 2005. 8871

Henze, D. K. and Seinfeld, J. H.: Global secondary organic aerosol from isoprene oxidation, Geophys. Res. Lett., 33, L09812, doi:10.1029/2006GL025976, 2006. 8858, 8859

Hilal, S. H., Carreira, L. A., and Karickhoff, S. W.: Prediction of the Vapor Pressure, Boiling Point, heat of Vaporization and Diffusion Coefficient of Organic Compounds, QSAR Comb. Sci., 22, 565–574, doi:10.1002/qsar.200330812, 2003. 8878

Hilal, S. H., Carreira, L. A., and Karickhoff, S. W.: Prediction of the Solubility, Activity Coefficient, Gas/Liquid and Liquid/Liquid Distribution Coefficients of Organic Compounds, QSAR Comb. Sci., 24, 709–720, doi:10.1002/qsar.200430866, 2004. 8878

Horowitz, L. W., Liang, J., Gardner, G. M., and Jacob, D. J.: Export of reactive nitrogen from North America during summertime: Sensitivity to hydrocarbon chemistry, J. Geophys. Res., 103, 13451–13476, 1998. 8859

Horowitz, L. W., Fiore, A. M., Milly, G. P., Cohen, R. C., Perring, A., Wooldridge, P. J., Hess, P. G., Emmons, L. K., and Lamarque, J. L.: Observational constraints on the chemistry of isoprene nitrates over the eastern United States, J. Geophys. Res., 112, D12S08, doi:10.1029/2006JD007747, 2007. 8859, 8864, 8868

Jang, M., Czoschke, N. M., Lee, S., and Kamens, R. M.: Heterogeneous Atmospheric Aerosol Production by Acid-Catalyzed Particle-Phase Reactions, Science, 298, 814–817, 2002. 8876

Jenkin, M. E., Hurley, M. D., and Wallington, T. J.: Investigation of the radical product channel of the $CH_3C(O)O_2$ + HO_2 reaction in the gas phase, Phys. Chem. Chem. Phys., 9, 3149–3162, doi:10.1039/b702757e, 2007. 8871

Kalberer, M., Paulsen, D., Saz, M., Steinbacher, M., Dommen, J., Prevot, A. S. H., Fisseha, R., Weingartner, E., Frankevich, V., Zenobi, R., and Baltensperger, U.: Identification of Polymers as Major Components of Atmospheric Organic Aerosols, Science, 303, 1659–1662, 2004. 8876

Kroll, J. H., Ng, N. L., Murphy, S. M., Flagan, R. C., and Seinfeld, J. H.: Secondary organic aerosol formation from isoprene photooxidation under high-NO_x conditions, Geophys. Res. Lett., 32, L18808, doi:10.1029/2005GL023637, 2005. 8859

Kroll, J. H., Ng, L. N., Murphy, S. M., Flagan, R. C., and Seinfeld, J. H.: Secondary Organic Aerosol Formation from Isoprene Photooxidation, Environ. Sci. Technol., 40, 1869–1877, 2006. 8859

Kwok, E. S. C. and Atkinson, R.: Estimatino of hydroxyl radical reaction rate constants for gas-phase organic compounds using a structure-reactivity relationship: an update, Atmos. Environ., 29, 1685–1695, 1995. 8870

Kwok, E. S. C., Aschmann, S. M., Arey, J., and Atkinson, R.: Product Formation from the Reaction of the NO_3 Radical with Isoprene and Rate Constants for the Reactions of Methacrolein and Methyl Vinyl Ketone with the NO_3 Radical, Int'l. J. Chem. Kin., 28, 925–934, 1996. 8864, 8869

Lelieveld, J., Butler, T. M., Crowley, J. N., Dillon, T. J., Fischer, H., Ganzeveld, L., Harder, H., Lawrence, M. G., Martinez, M., Taraborrelli, D., and Williams, J.: Atmospheric oxidation capacity sustained by a tropical forest, Nature, 452, 737–740, doi:10.1038/nature06870, 2008. 8871

Müller, L., Reinnig, M.-C., Warnke, J., and Hoffmann, Th.: Unambiguous identification of esters as oligomers in secondary organic aerosol formed from cyclohexene and cyclohexene/a-pinene ozonolysis, Atmos. Chem. Phys., 8, 1423–1433, 2008, http://www.atmos-chem-phys.net/8/1423/2008/. 8876

Munger, J. W., Wofsy, S. C., Bakwin, P. S., Fan, S.-M., Goulden, M. L., Daube, B. C., and Goldstein, A. H.: Atmospheric deposition of reactive nitrogen oxides and ozone in a temperate deciduous forest and a subarctic woodland. 1. Measurements and mechanisms, J. Geophys. Res., 101, 12639–12657, 1996. 8879

Ng, N. L., Kwan, A. J., Surratt, J. D., Chan, A. W. H., Chhabra, P. S., Sorooshian, A., Pye, H. O. T., Crounse, J. D., Wennberg, P. O., Flagan, R. C., and Seinfeld, J. H.: Secondary organic aerosol (SOA) formation from reaction of isoprene with nitrate radicals (NO_3), Atmos. Chem. Phys., 8, 4117–4140, 2008, http://www.atmos-chem-phys.net/8/4117/2008/. 8859, 8860, 8870, 8871, 8873, 8874, 8877

Noda, J., Nyman, G., and Langer, S.: Kinetics of the Gas-Phase Reaction of Some Unsaturated Alcohols with the Nitrate Radical, J. Phys. Chem. A, 106, 945–951, 2002. 8870

Odum, J. R., Hoffmann, T., Bowman, F., Collins, D., Flagan, R. C., and Seinfeld, J. H.: Gas/Partitioning and Secondary Organic Aerosol Yields, Environ. Sci. Technol., 30, 2580–2585, 1996. 8875

Olivier, J. G. J., Van Aardenne, J. A., Dentener, F. J., Pagliari, V., Ganzeveld, L. N., and Peters, J. A. H. W.: Recent trends in global greenhouse gas emissions: regional trends 1970-2000 and spatial distribution of key sources in 2000, Environ. Sci., 2, 81–99, 2005. 8858

Pankow, J. F. and Asher, W. E.: SIMPOL.1: a simple group contribution method for predicting vapor pressures and enthalpies of vaporization of multifunctional organic compounds, Atmos. Chem. Phys., 8, 2773–2796, 2008, http://www.atmos-chem-phys.net/8/2773/2008/. 8874

Perring, A. E., Wisthaler, A., Graus, M., Wooldridge, P. J., Lockwood, A. L., Mielke, L. H., Shepson, P. B., Hansel, A., and Cohen, R. C.: A product study of the isoprene+NO3 reaction, Atmos. Chem. Phys. Discuss., 9, 5231–5261, 2009, http://www.atmos-chem-phys-discuss.net/9/5231/2009/. 8868, 8869, 8873

Ridley, B. A., Grahek, F. E., and Walega, J. G.: A Small, High-Sensitivity, Medium-Response Ozone Detector Suitable for Measurements from Light Aircraft, J. Atmos. Ocean. Tech., 9, 142–149, 1992. 8862

Rohrer, F., Bohn, B., Brauers, T., Brüning, D., Johnen, F.-J., Wahner, A., and Kleffmann,

J.: Characterisation of the photolytic HONO-source in the atmosphere simulation chamber SAPHIR, Atmos. Chem. Phys., 5, 2189–2201, 2005, http://www.atmos-chem-phys.net/5/2189/2005/. 8861

Sandu, A. and Sander, R.: Technical note: Simulating chemical systems in Fortran90 and Matlab with the Kinetic PreProcessor KPP-2.1, Atmos. Chem. Phys., 6, 187–195, 2006, http://www.atmos-chem-phys.net/6/187/2006/. 8863

Saunders, S. M., Jenkin, M. E., Derwent, R. G., and Pilling, M. J.: Protocol for the development of the Master Chemical Mechanism, MCM v3 (Part A): tropospheric degradation of non-aromatic volatile organic compounds, Atmos. Chem. Phys., 3, 161–180, 2003, http://www.atmos-chem-phys.net/3/161/2003/. 8863

Seinfeld, J. H. and Pandis, S. N.: Atmospheric Chemistry and Physics: From Air Pollution to Climate Change, 1998. 8879

Shepson, P. B., Mackay, E., and Muthuramu, K.: Henry's Law Constants and Removal Processes for Several Atmospheric β-Hydroxy Alkyl Nitrates, Environ. Sci. Technol., 30, 3618–3623, 1996. 8878, 8879

Skov, H., Hjorth, J., Lohse, C., Jensen, N. R., and Restelli, G.: Products and mechanisms of the reactions of the nitrate radical (NO_3) with isoprene, 1,3-butadiene and 2,3-dimethyl-1,3-butadiene in air, Atmos. Environ., 26A, 2771–2783, 1992. 8860, 8868, 8869, 8873

Starn, T. K., Shepson, P. B., Bertman, S. B., Riemer, D. D., Zika, R. G., and Olszyna, K.: Nighttime isoprene chemistry at an urban-impacted forest site, J. Geophys. Res., 103, 22437–22447, 1998. 8859

Steinbacher, M., Dommen, J., Ordonez, C., Reimann, S., Grüebler, F. C., Staehelin, J., Andreani-Aksoyoglu, S., and Prevot, A. S. H.: Volatile Organic Compounds in the Po Basin. Part B: Biogenic VOCs, J. Atmos. Chem., 51, 293–315, doi:10.1007/s10874-005-3577-0, 2005. 8859

Stroud, C. A., Roberts, J. M., Williams, E. J., D., H., Angevine, W. M., Fehsenfeld, F. C., Wisthaler, A., Hansel, A., Martinez-Harder, M., Harder, H., Brune, W. H., Hoenninger, G., Stutz, J., and White, A. B.: Nighttime isoprene trends at an urban forested site during the 1999 Southern Oxidant Study, J. Geophys. Res., 107(D16), 4314, doi:10.1029/2001JD000959, 2002. 8859

Suh, I., Lei, W., and Zhang, R.: Experimental and Theoretical Studies of Isoprene Reaction with NO_3, J. Phys. Chem. A, 105, 6471–6478, 2001. 8860

Surratt, J. D., Murphy, S. M., Kroll, J. H., Ng, N. L., Hildebrandt, L., Sorooshian, A., Szmigielski,

R., Vermeylen, R., Maenhaut, W., Clayes, M., Flagan, R. C., and Seinfeld, J. H.: Chemical Composition of Secondary Organic Aerosol Formed from the Photooxidation of Isoprene, J. Phys. Chem. A, 110, 9665–9690, 2006. 8876

Thornton, J. A., Wooldridge, P. J., and Cohen, R. C.: Atmospheric NO_2, in Situ laser-Induced Fluorescence Detection at Parts per Trillion Mixing Ratios, Anal. Chem., 72, 528–539, 2000. 8862

Thornton, J. A., Wooldridge, P. J., Cohen, R. C., Martinez, M., Harder, H., Brune, W. H., Williams, E. J., Roberts, J. M., Fehsenfeld, F. C., Hall, S. R., Shetter, R. E., Wert, B. P., and Fried, A.: Ozone production rates as a function of NO_x abundances and HO_x production rates in the Nashville urban plume, J. Geophys. Res., 107(D12), 4146, doi: 10.1029/2001JD000932, 2002. 8858, 8871

Treves, K. and Rudich, Y.: The Atmospheric Fate of C_3-C_6 Hydroxyalkyl Nitrates, J. Phys. Chem. A., 107, 7809–7817, 2003. 8878

Turnipseed, A. A., Huey, L. G., Nemitz, E., Stickel, R., Higgs, J., Tanner, D. J., Slusher, D. L., Sparks, J. P., Flocke, F., and Guenther, A.: Eddy covariance fluxes of peroxyacetyl nitrates (PANs) and NO_y to a coniferous forest, J. Geophys. Res., 111, D09304, doi: 10:1029/2005JD006631, 2006. 8879

Vaughan, S., Canosa-Mas, C., Pfrang, C., Shallcross, D., Watson, L., and Wayne, R.: Kinetic studies of reactions of the nitrate radical (NO_3) with peroxy radicals (RO_2): an indirect source of OH at night?, Phys. Chem. Chem. Phys., 8, 3749–3760, doi:10.1039/b605569a, 2006. 8871

von Kuhlmann, R., Lawrence, M. G., Pöschl, U., and Crutzen, P. J.: Sensitivities in global scale modeling of isoprene, Atmos. Chem. Phys., 4, 1–17, 2004, http://www.atmos-chem-phys.net/4/1/2004/. 8859

Wegener, R., Brauers, T., Koppmann, R., Bares, S. R., Roher, F., Tillmann, R., Wahner, A., Hansel, A., and Wisthaler, A.: Simulation chamber investigation of the reactions of ozone with short-chained alkenes, J. Geophys. Res., 112, D13301, doi:10.1029/2006JD007531, 2007. 8861

Wille, U., Becker, E., Schindler, R. N., Lancer, I. T., Poulet, G., and Le Bras, G.: A Discharge Flow Mass-Spectrometric Study of the Reaction Between the NO_3 Radical and Isoprene, J. Atmos. Chem, 13, 183–193, 1991. 8860

Wolfe, G. M., Thornton, J. A., Yatavelli, R. L. N., McKay, M., Goldstein, A. H., LaFranchi, B., Min, K.-E., and Cohen, R. C.: Eddy covariance fluxes of acyl peroxy nitrates (PAN, PPN and

MPAN) above a Ponderosa pine forest, Atmos. Chem. Phys., 9, 615–634, 2009, http://www.atmos-chem-phys.net/9/615/2009/. 8879

Wu, S., Mickley, L. J., Jacob, D. J., Logan, J. A., Yantosca, R. M., and Rind, D.: Why are there large differences between models in global budgets of tropospheric ozone?, J. Geophys. Res., 112, D05302, doi:10.1027/2006JD007801, 2007. 8858, 8859

Zhang, Y., Huang, J. P., Henze, D. K., and Seinfeld, J. H.: Role of isoprene in secondary organic aerosol formation on a regional scale, J. Geophys. Res., 112, D20207, doi:10.1029/2007JD008675, 2007. 8859

Table 1. Gas phase reactions and rates included in reduced isoprene chemistry model.

rxn #	reaction	rate at 298 K (cm^3 s^{-1})	reference
1	C5H8+NO_3 →NISOPO2	6.78×10^{-13}	MCM V3.1
2	NISOPO2+NO_3 →0.70NIT1+0.035 MVK+0.035 MACR +1.25 NO_2+0.80 HO_2	2.5×10^{-12}	MCM V3.1
3	NISOPO2+HO_2 →0.70NIT1+0.035 MVK+0.035 MACR +0.25 NO_2+0.80 HO_2	2.3×10^{-11}	MCM V3.1
4	NISOPO2+RO_2 →0.70NIT1+0.035 MVK+0.035 MACR +0.25 NO_2+0.80 HO_2	1.30×10^{-12}	MCM V3.1
5	NIT1+NO_3 →NIT1NO3OO	7×10^{-14}	fit
6	NIT1NO3OO+NO_3 →0.6 NIT2+0.4 NIT3+NO_2+0.8 HO_2	2.5×10^{-12}	MCM V3.1
7	NIT1NO3OO+HO_2 →0.6 NIT2+0.4 NIT3+0.8 HO_2	2.3×10^{-11}	MCM V3.1
8	NIT1NO3OO+RO_2 →0.6 NIT2+0.4 NIT3+0.8 HO_2	1.30×10^{-12}	MCM V3.1
9	NIT1+O_3 → NIT4	3×10^{-18}	fit (assumed $4.3\times10^{-5}\times k_5$)

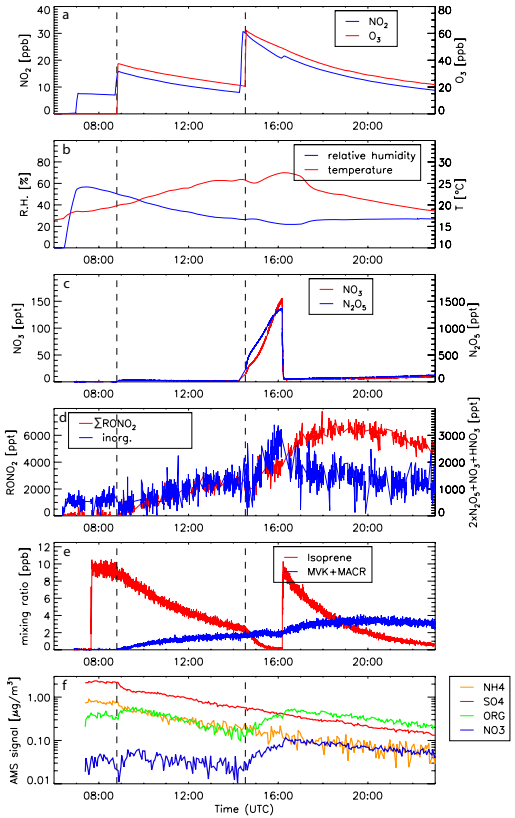

Fig. 1. Descending top to bottom, measurements of **(a)** NO_2 and O_3 (CL measurement), **(b)** chamber temperature and relative humidity (RH), **(c)** NO_3 and N_2O_5 (CaRDS), **(d)** organic nitrates ($RONO_2$) and inorganic nitrates (NO_3+2×N_2O_5+HNO_3) (TD-LIF), **(e)** isoprene and the sum of methacrolein and methyl vinyl ketone (PTR-MS), and **(f)** AMS measurements of aerosol composition.

ACPD
9, 8857–8902, 2009

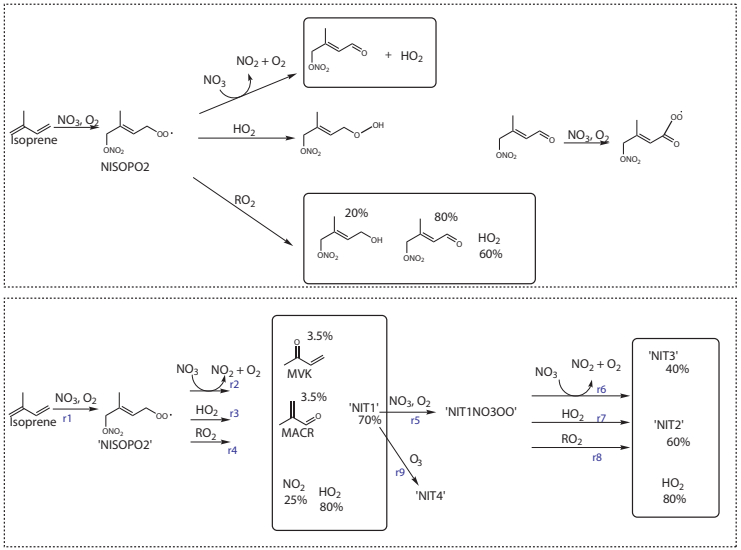

Fig. 2. Top: schematic of isoprene+NO_3 mechanism MCM V3.1. 100% of first generation oxidation products are alkyl nitrates. The only first generation product which is reactive towards NO_3 is the carbonyl nitrate, which reacts in an aldehyde+NO_3 mechanism at a rate of 1.1×10^{-14} cm^3 $s-1$. Bottom: the modified mechanism used in this study. NIT1–NIT4 are lumped species representing organic nitrates produced by the first (NIT1) and second (NIT2, NIT3, NIT4) oxidation steps. NIT1 has one $RONO_2$ group and one carbon-carbon double bond. Oxidation of the second double bond by NO_3 is presumed to either leave the original nitrate functionality (NIT2) or add an additional $RONO_2$ group (NIT3). Oxidation of NIT1 by O_3 is presumed to leave the nitrate functionality (NIT4). NIT1NO3OO is the peroxy radical generated by reaction of NIT1 with NO_3 followed by O_2.

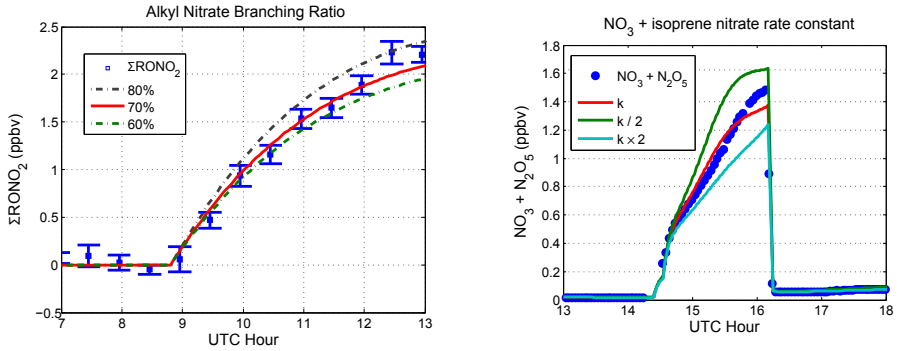

Fig. 3. Left: model with varying branching ratios for production of alkyl nitrates from the initial isoprene+NO_3 reaction. Error bars represent $\pm 2\sigma$ of TD-LIF measurement. Right: NOAA N_2O_5 and model calculations using $k = 7.0 \times 10^{-14}$ for NO_3+isoprene.

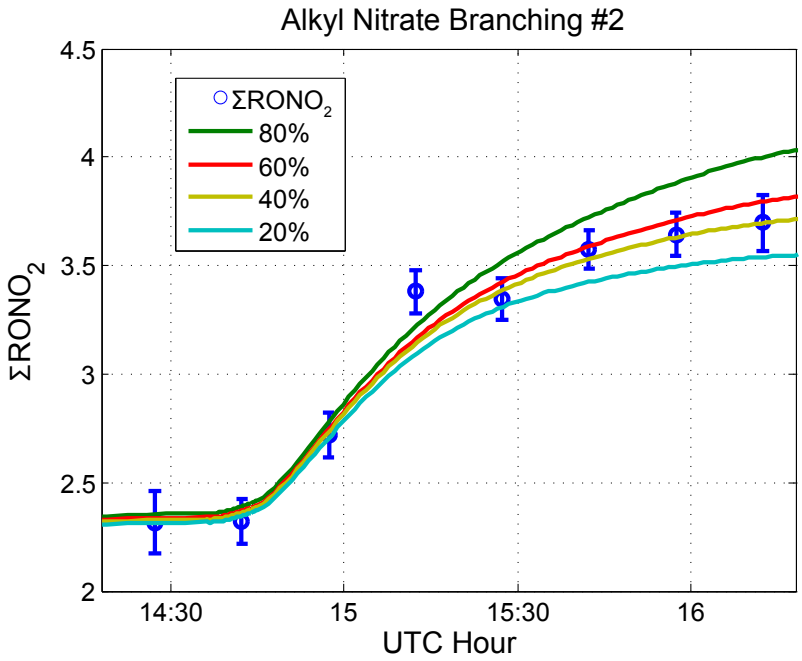

Fig. 4. Model runs varying the branching ratio to form alkyl nitrates from the oxidation of isoprene's second double bond.

ACPD
9, 8857–8902, 2009

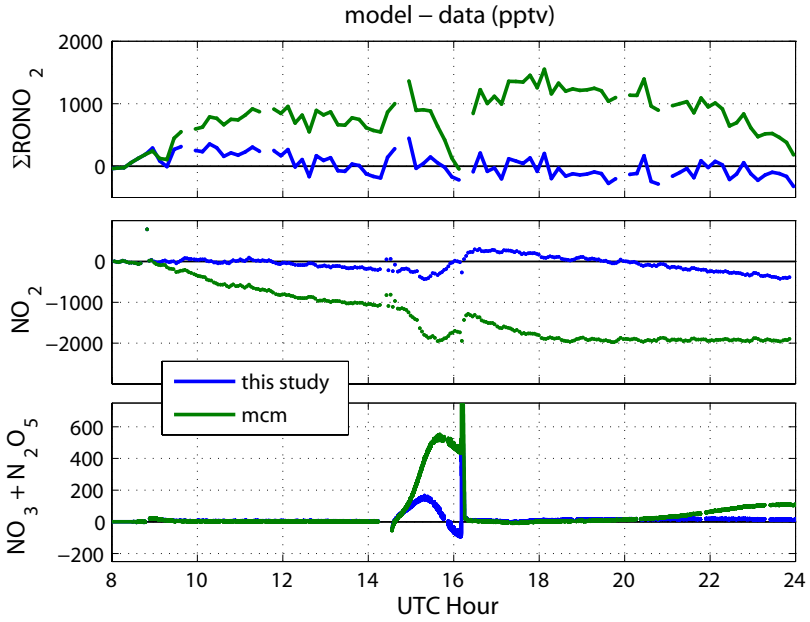

Fig. 5. Differences between data and model (data-model) for (top) $\Sigma RONO_2$, (middle) NO_2, and (bottom) $NO_3+N_2O_5$. Green lines are calculations from MCM V3.1 and blue lines are the modified model from this work.

ACPD
9, 8857–8902, 2009

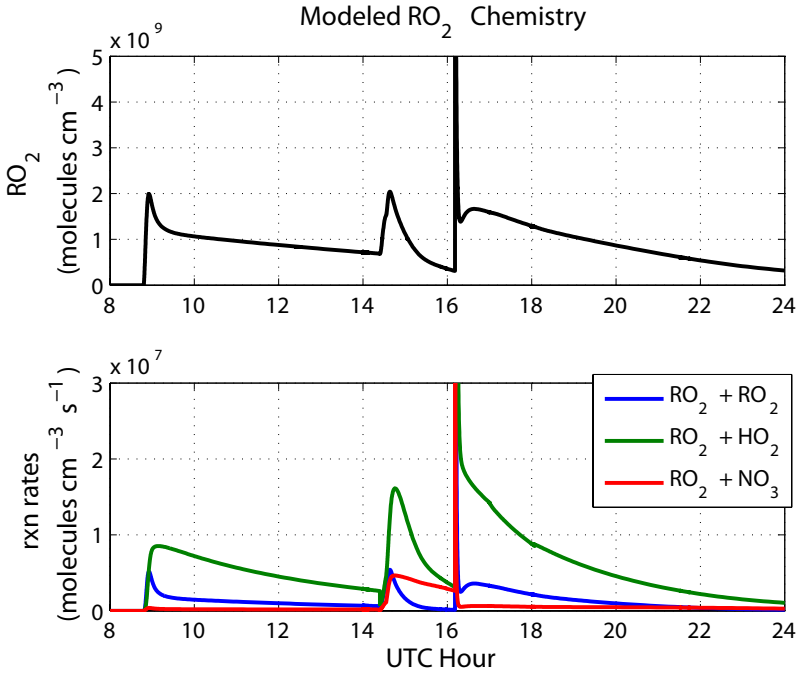

Fig. 6. Modeled calculations of (top) total peroxy radicals concentrations, and (bottom) sum of the rates of all RO_2+RO_2 reactions (blue), all RO_2+HO_2 reactions (green) and all RO_2+NO_3 reactions (red).

ACPD
9, 8857–8902, 2009

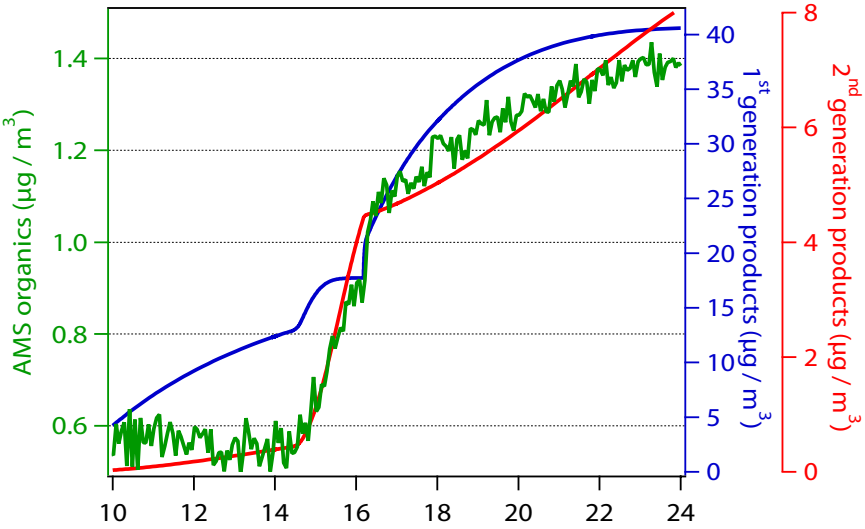

Fig. 7. Wall loss corrected AMS organics (green line, left axis), the modeled first generation oxidation products (blue line) and second generation oxidation products (red). Modeled first and second generation products are both expressed in units of $\mu g/m^3$ of the initial isoprene reacted, calculated as moles/m^3 of product × the molecular weight of isoprene, allowing the mass yield ($\Delta VOC/\Delta SOA$) from each step to be calculated by comparing the product mass to measured organic aerosol mass.

ACPD
9, 8857–8902, 2009

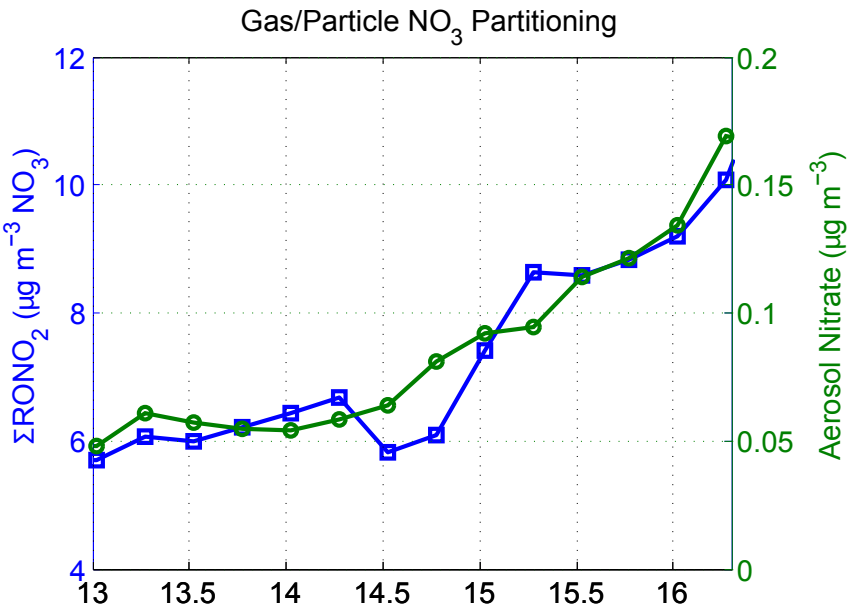

Fig. 8. Increases in TDLIF gas+aerosol $RONO_2$ (blue) and AMS nitrate (green) during the second oxidation step in the chamber. AMS and TDLIF data are mapped to the same time resolution using 15 min means.

ACPD
9, 8857–8902, 2009

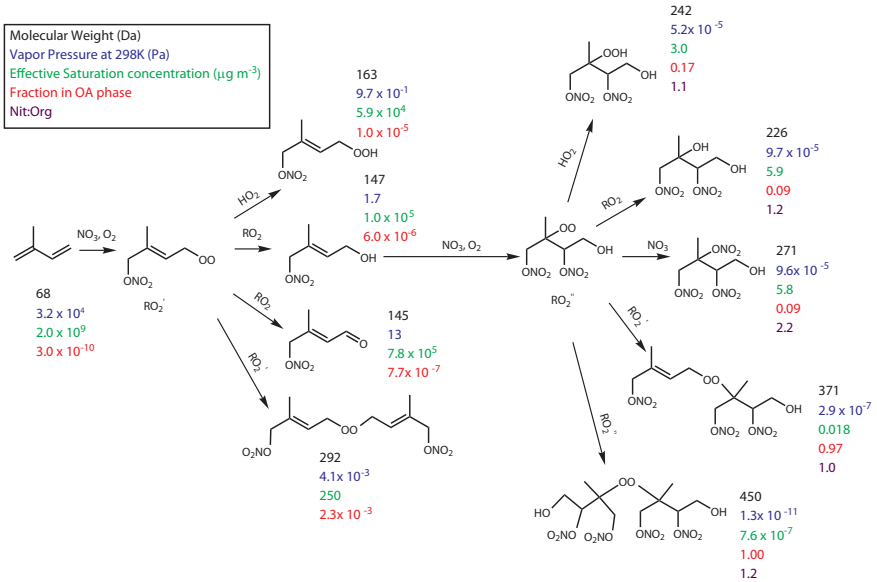

Fig. 9. The molecular weight (Da, black), vapor pressure (Torr, blue), effective saturation (μg/m^3, green) equilibrium partitioning in OA phase at 0.6 μg/m^3, and nitrate:organic ratio of the expected products of two stages of isoprene oxidation by NO_3.

ACPD
9, 8857–8902, 2009

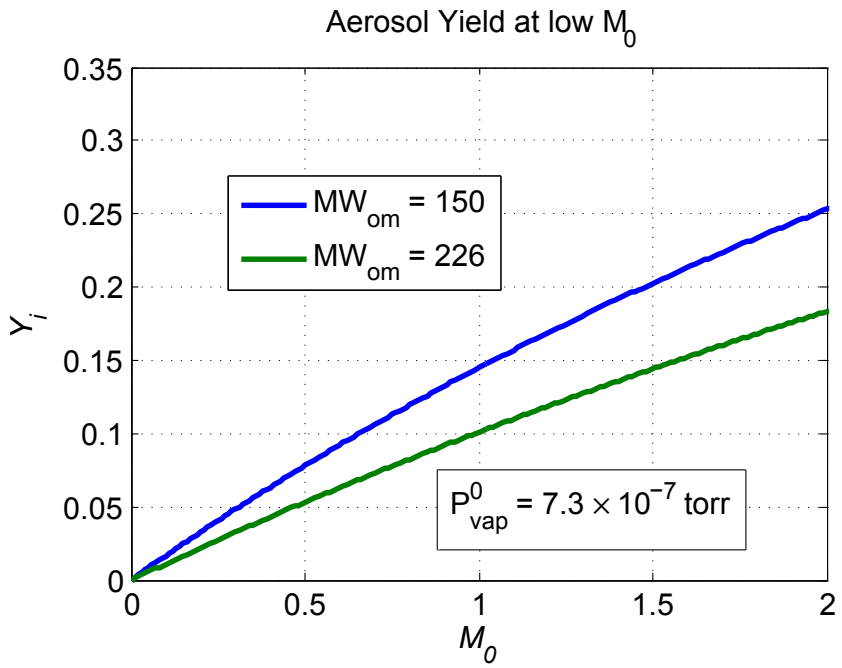

Fig. 10. Theoretical mass yields of SOA as a function of total OA loading and OA mean molecular weight.

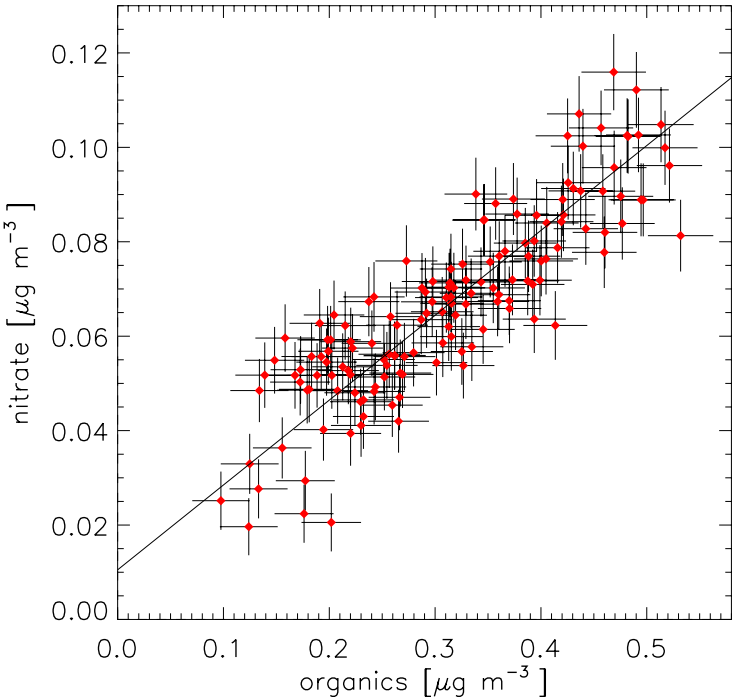

Fig. 11. AMS organic aerosol vs AMS nitrate aerosol following 14:15 UTC. A linear fit to the data yields a slope of 0.180±0.007, R^2=0.76, χ^2/N=1.19.

ACPD
9, 8857–8902, 2009

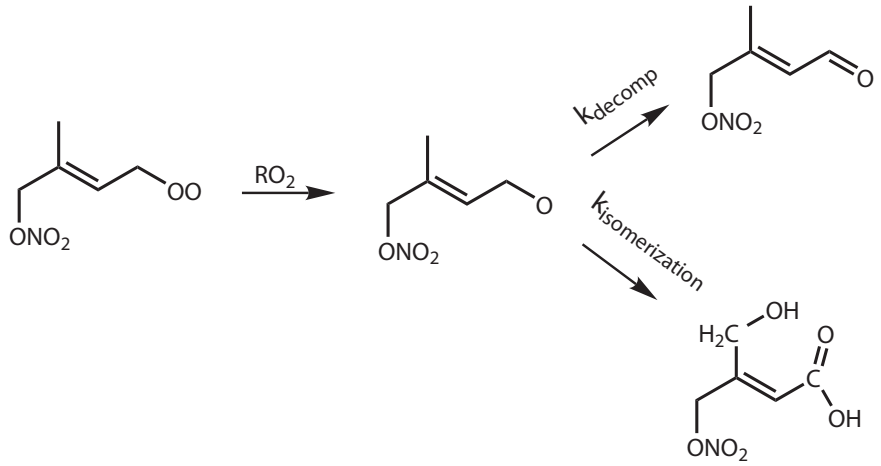

Fig. 12. Isomerization vs. decomposition of the nitrate oxy radical. Multiple steps in the isomerization channel are left out of diagram for simplicity. Only final stable products are shown.